Sensors & Actuators: B. Chemical 321 (2020) 128463

Contents lists available at ScienceDirect

Sensors and Actuators B: Chemical

journal homepage: www.elsevier.com/locate/snb

U-bent fiber optic plasmonic biosensor platform for ultrasensitive analyte detection

Ramakrishna Bandaru[a,1], Divagar M[a,b], Shruti Khanna[c], Christina Grace Danny[d], Shalini Gupta[c], Vani Janakiraman[b], V V R Sai[a,*]

[a] Biomedical Engineering Laboratory, Department of Applied Mechanics, Indian Institute of Technology Madras, Chennai 600036, India
[b] Department of Biotechnology, Indian Institute of Technology Madras, Chennai 600036, India
[c] Department of Chemical Engineering, Indian Institute of Technology Delhi, New Delhi 110016, India
[d] Department of Electronics and Instrumentation Engineering, MSRIT, Bengaluru, Karnataka 560054, India

ARTICLE INFO

Keywords:
Fiber optic biosensor
Gold nanoparticles
Plasmonic labels
Evanescent wave absorbance
Attomolar analyte detection

ABSTRACT

This study demonstrates a rapid, wash-free, dip-type plasmonic fiberoptic absorbance biosensor (P-FAB) capable of zeptomole analyte detection and 6-orders of wide dynamic range. It involves a sandwich immunoassay on a compact U-bent fiber optic probe surface that works by dipping an antibody-functionalized probe into a mixture of sample and gold nanoparticle (AuNP) label suspension. The U-bent fiberoptic probes with a high evanescent wave absorbance sensitivity allow detection of the high extinction AuNP labels measured in terms of light intensity change using a pair of LED and photodetector (PD). This simple and low-cost P-FAB gives an unprecedented detection limit of 0.17 zeptomole for human immunoglobulin G (HIgG) in 25 μL buffer in just 25 min. Further silver enhancement of AuNP labels for 5 min results in a limit of quantitation (LoQ) down to 0.17 zeptomole (~100 – 150 molecules in 25 μL), making P-FAB a highly sensitive and low-cost technology for point-of-care diagnostics.

1. Introduction

Ultra-sensitive and rapid analyte detection down to attomolar concentrations at point-of-care offers several possibilities including (i) early diagnosis of certain critical diseases such as myocardial infarction, cancer and tuberculosis and the disease prognosis [1] (ii) detection of analytes of interest from very small volumes of serum/plasma, and (iii) exploration of body fluids such as saliva, urine, sweat etc as a safe alternative to blood samples. Lateral flow assay (LFA) technology, relying on plasmonic sandwich immunoassays, remains as a highly successful point-of-care (PoC) diagnostic technology [2] due to their exceptional features such as low-cost, rapid analysis and naked eye detection of biomarkers. Despite its well-known advantages as mentioned-above, LFA technology suffers several constraints, including low sensitivity, inability to quantify specific and non-specific binding, and requirement of a separate reader instrument that limit its scope mostly to semi-quantitative analysis [3]. Several attempts have been made to improve their sensitivity, including silver enhancement by exploiting the catalytic properties of AuNP labels [4–7] and by utilizing fluorescent labels [8] and an analyte detection limit down to pg/mL or several femtomolar concentrations was realized [9]. Besides enhanced sensitivity, the need for the hour demands detection of further ultra-low analyte concentrations, which is crucial in specific disease conditions like early-stage cancer. In addition, an ideal PoC device is expected not only to inherit the simplicity in sensing methodology but also to meet the ASSURED criterion for PoC devices recommended by World Health Organization (WHO) [10].

To aid in the realization of ASSURED PoC devices, it is important to realize a suitable, highly sensitive and yet simple transduction system in order to improve the sensitivity without any washing and signal amplification steps. Here, we propose to exploit fiber optic transducers that offer several advantages including (i) simpler optical coupling and compact configuration at a lower cost in comparison to bulk optical set-up, (ii) an efficient excitation of plasmonic nanostructures by means of evanescent waves over the decladded fibers and (iii) large dynamic range and recent advances in optoelectronics. We propose a wash-free, dip-type plasmonic fiberoptic absorbance biosensor dubbed P-FAB, that exploits an excellent combination of plasmonic labels with high extinction coefficient and U-bent fibreoptic transducer probes with high absorbance sensitivity to achieve a zeptomole analyte detection in

* Corresponding author.
E-mail address: vvrsai@iitm.ac.in (S. V V R).
[1] Currently affiliated to SRM Institute of Science and Technology, Kattankulathur, Chennai – 603203.

https://doi.org/10.1016/j.snb.2020.128463
Received 7 April 2020; Received in revised form 16 May 2020; Accepted 12 June 2020
Available online 15 June 2020
0925-4005/

sandwich assay format. Previously, our group has reported a proof-of-concept plasmonic sandwich assay on the surface of a U-bent fibreoptic sensor probe with 13 nm AuNP labels, and an optical setup consisting of a broadband LED and a fiberoptic spectrometer [11]. In this study, we illustrate an even higher sensitivity and rapid analyte detection assay by adopting the following conditions for the sensing scheme: (i) larger sized AuNP labels (40–60 nm) to increase the optical absorbance associated with each sandwich immunocomplex [12], (ii) a green LED and photodetector for sensitive measurement of light intensity variation through the fiber probe due to the presence of AuNP labels, (iii) an optional absorbance signal amplification step by silver staining the AuNP labels and, (iv) rapid analyte detection using AuNP labels also as analyte carriers, where the probe is exposed to analyte-antibody-AuNP label complex instead of the conventional sequential sandwich assay format.

2. Experimental section

The experimental methods including the U-bent fiber optic probe fabrication and its biofunctionalization with capture antibodies, AuNP conjugation with detection antibodies, optical setup, sandwich assay procedure, silver staining protocol, and the positive control BIAcore SPR experiments are all described in the supplementary section of this manuscript.

3. Results and discussion

3.1. Ultrasensitive detection of AuNP labels by U-bent fiberoptic sensor probes

A compact U-bent probe (Fig. 1A), fabricated by decladding and bending a fused silica fiber (200 μm core) under butane flame to obtain a bend diameter of 1.5 mm, efficiently converts a large number of lower order modes (concentrated around the optical axis) into higher order modes. This allows a large fraction of light to be available at the core surface and improves the EW-based light-matter interaction at the core-medium interface in the bent region. Numerical simulations (refer to SI) for the light propagation in the U-bent probe using ray optics approach show an increase in the evanescent power availability (Fig. 1B). Acute bending of an otherwise straight optical fiber (to a radius of curvature less than five times the fiber core radius, as in this study) leads to a significant modification of the local core refractive index due to compressive and tensile strains along the inner and outer curvatures of the U-shaped region respectively. The local numerical aperture tends to drop exponentially from the outer curvature and remains zero for the rest of the fiber core. As a consequence, the rays propagate along the outer curvature with propagation width close to less than one-tenth of the radius, similar to whispering gallery rays [13]. Thus, a large fraction of light is available at the core surface for EW based light-AuNP interaction. This results in probes with significantly higher absorbance sensitivity [14,15] that allow detection of even a small number of surface-bound AuNPs. The presence of AuNPs on the fiber core surface in the bent region gives rise to a significant loss in the optical power at the other end of the U-bent of the probe (see Fig. 1C) due to EW based light-particle interaction. On the other hand, the unbound AuNPs floating in the medium do not elicit any response as EW is a near-field phenomenon with its depth of penetration limited to the order of wavelength of light.

To demonstrate the efficiency of U-bent probes, amine functionalized U-bent probes were exposed to AuNP suspension, and the drop in light intensity at the photodetector (PD) end was monitored over time. Fig. 1C shows the real-time absorbance response due to the formation of a chemisorbed monolayer of AuNPs measured using a narrow-band green light source (laser at 532 nm) and a photodetector (PM100, Thorlabs Inc. USA). By leveraging the high absorbance sensitivity of the probes and the large dynamic range of the photodetector, a drop in light intensity over four orders was observed for a saturated surface coverage (~150 particle/μm^2) while the lowest AuNP surface density of 6–7 particles/μm^2 also led to a significant rise in absorbance of 0.1 units (Fig. 1C). Thus, these results showed that the probe absorbance response varies proportionally to the surface density of the AuNP labels.

Subsequently, a direct immunoassay was realized to establish a proof-of-concept for an assay with AuNP labels as well as to understand the influence of the AuNP concentration on the total assay time and the magnitude of the sensor response (Fig. S3). For this purpose, U-bent fiber probes were functionalized with HIgG and subjected to different concentrations of goat anti-human IgG (aHIgG, F_c specific) antibody-conjugated AuNP labels (AuNP reagent). A saturated absorbance response of ~ 2 units was obtained with 10× AuNP concentration within 20 min (bare AuNP OD_{530nm} = 0.75 A.U.), while 5×, 2× and 1× reagents showed ~77 %, 19 % and 8% of response respectively compared to 10× concentration. These results demonstrated a high sensitivity of the U-bent probes for a direct immunoassay with plasmonic AuNP labels.

3.2. Realization of P-FAB based sandwich immunosensor

A two-step sandwich assay was carried out on our P-FAB for analyte detection (Fig. 2A). As the first step, HIgG target analyte was first captured onto F_c specific aHIgG conjugated AuNP labels, to reduce the assay time by exploiting a liquid phase homogeneous reaction. AuNP reagent (10×, 25 μL) containing a total number of ~1.5 × 10^{10} AuNPs (ca. 50 antibodies per AuNP) was added to a sample volume of 25 μL containing 10 pg/mL (70 fM) [16] of HIgG analyte (10^6 molecules) in a 0.2 mL microcentrifuge tube. A high concentration of AuNP reagent nullifies any hook effect [17] and ensures at least one AuNP for each analyte molecule to form HIgG-aHIgG-AuNP immunocomplex for their detection. In the second step, a U-bent fiberoptic probe functionalized with F_{ab} specific aHIgG was dipped into the microcentrifuge tube to allow the formation of sandwich immunocomplexes on a fiber probe surface. The absorbance of light due to the presence of AuNP labels was monitored using a pair of narrowband green LED and a PD (Figs. 2A and S2). Fig. 2C shows the temporal response obtained from a probe subjected to an analyte concentration of 10 pg/mL over 20 min.

Subsequently, silver enhancement over AuNP labels by catalytic reduction was adopted to amplify the plasmonic absorbance response [18,19]. Probes were silver stained by dipping them in phosphate buffer saline (PBS) twice followed by a mixture of silver enhancer and precursor solution (Sigma Chemicals, USA) in 1:1 v/v ratio for 15 min (Fig. 2B). Fig. 2C shows an exponential rise in absorbance response for the first 5 min followed by saturation at the end of 15 min. Scanning electron microscope (SEM) images showed a controlled growth of silver over AuNP forming islands as large as 5 times the size of AuNP in the initial 5 min, followed by uncontrolled, non-specific silver deposition due to photocatalysis at later time points (Fig. S4). Silver staining for 5 min consistently gave reliable amplification of the sensor response.

3.3. P-FAB dose response for human IgG

Further, the sensitivity, dynamic range and detection limits of P-FAB were evaluated. The aHIgG (F_{ab} specific) functionalized U-bent probes (> 25 no's) having a similar sensitivity (details in methods section, SI) were exposed to analyte concentrations over the range of 1 fg/mL (7 aM) to 1 ng/mL (7 pM) of HIgG (containing a total of ~10^2 to ~10^8 molecules, respectively) in addition to control (0 fg/mL). The P-FAB results showed a distinct response proportional to the analyte concentration (n = 3) at the end of 20 min (Figs. 3A and S5). The sensor response at the end of 20 min was taken instead of steady state mainly for a rapid analyte detection. Absorbance response from control probes without HIgG was 0.047 ± 0.005, which was considerably lower than 0.074 ± 0.009 obtained for 1 fg/mL. It is interesting to note that the response due to non-specific binding of PEGylated aHIgG-AuNP

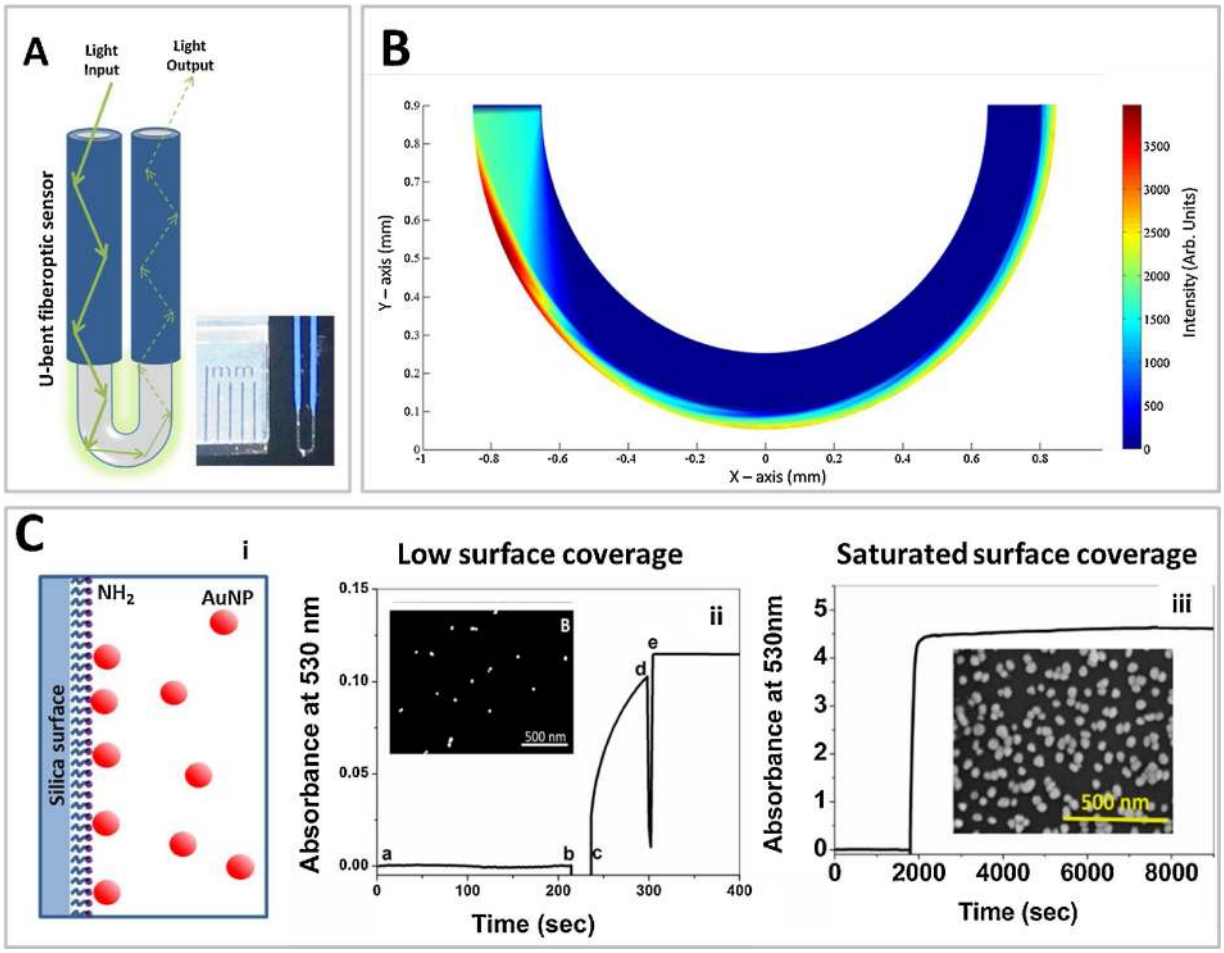

Fig. 1. (A) Schematic showing the working principle of P-FAB and an actual image of a U-bent fiberoptic probe (200 μm fiber silica core, 1.5 mm bend diameter). The optical power loss in the U-bent region due to EW based absorbance by the AuNP bound to the probe surface is depicted in terms of thickness of the light ray. (B) Numerical simulations using ray-optics approach showing light propagation in an acute U-bent optical fiber probe along its outer curvature similar to whispering gallery rays. (C) (ii) Low surface coverage and (iii) saturated surface coverage and the corresponding EW based absorbance response due to chemisorption of AuNP to amino-silanized U-bent fiber probe surface. (ii) Temporal response obtained from a U-bent probe exposed to 1× concentration of AuNP over a duration of 60 s. The absorbance response from amine functionalized probe was introduced into a vial containing DI water at point 'a' as a reference and a stable response was observed until point 'b' before withdrawing from DI water and introducing it into a 1× diluted AuNP solution at point 'c.' AuNP chemisorption to the U-bent probes was allowed till an absorbance response up to 0.1 units was observed (point 'd') and immediately withdrawn and reintroduced into DI water (point e). Inset: A scanning electron microscopic image showing a low and dense surface coverage of AuNPs on the fiber surface.

(control) was less than 2.5 % of the maximum possible absorbance response due to the specific binding observed in Fig. 1C. The analyte dose response showed a linear increase in absorbance between 1 fg/mL and 1 pg/mL with a sensitivity of 0.0148 A_{530nm}/log (fg/mL) (R^2 = 0.98) (Fig. 3C). The sensor was able to consistently detect analyte concentrations as low as 1 fg/mL (LoD, ~7 aM or 0.17 zeptomole in 25 μL). However, the LoQ based on the response, defined as 10σ above the mean blank (control) value, corresponded to 100 fg/mL. Hence, P-FAB with plasmonic labels alone offered 4-orders of dynamic range starting from 100 fg/mL (0.7 fM) to 1 ng/mL (7 pM). (Fig. 3C). In general, the analyte dose response from a sensor is anticipated to be typically a sigmoidal curve. It may be noted that the sensor response from Fig. 3C appears as only the lower half of such a sigmoid curve for the analyte concentrations investigated here. An extrapolation of the response curve can reveal the sensor's ability to respond to analyte concentrations much greater than 1 ng/mL, however, for which much simpler and cost-effective technologies such as LFA are already available.

Absorbance signal amplification by silver staining of AuNP labels on the fiber probes further confirmed the zeptomole analyte detection limit of P-FAB. Upon 5 min of silver staining, an exponential increase in the real-time absorbance response proportional to the analyte concentration was obtained as shown in Fig. 3B. While the control probe gave an absorbance of 0.337 ± 0.017, a significantly higher response of 0.552 ± 0.03 was obtained for probes treated with 1 fg/mL analyte concentration. It is evident from Fig. 3A that the response is similar to a step response of a first order system, whereas the Fig. 3B shows an exponentially rising trend mostly caused by the avalanche process of Ag reduction around AuNP islands. The improvement in the sensitivity and linearity of sensor response after the silver enhancement is attributed to an exponential multiplication factor in the absorbance response caused by the avalanche of Ag reduction. For the analyte concentrations under investigation, an absorbance sensitivity of ~ 0.281 A_{530nm}/log (fg/mL) (R^2 = 0.91) was observed, which was ~19 times higher than the sensitivity obtained with plasmonic labels alone (Fig. 3D). The results from silver enhancement demonstrated a significant improvement in LoQ down to 1 fg/mL. For analyte concentrations higher than 1 pg/mL, a large standard deviation in the absorbance response was observed. This could be attributed to a wider distribution in the probable number of bound AuNP labels for higher analyte concentrations, which results in a wide variation in the absorbance response upon amplification by a large factor of ~20. Hence, silver enhancement could be most suitable to

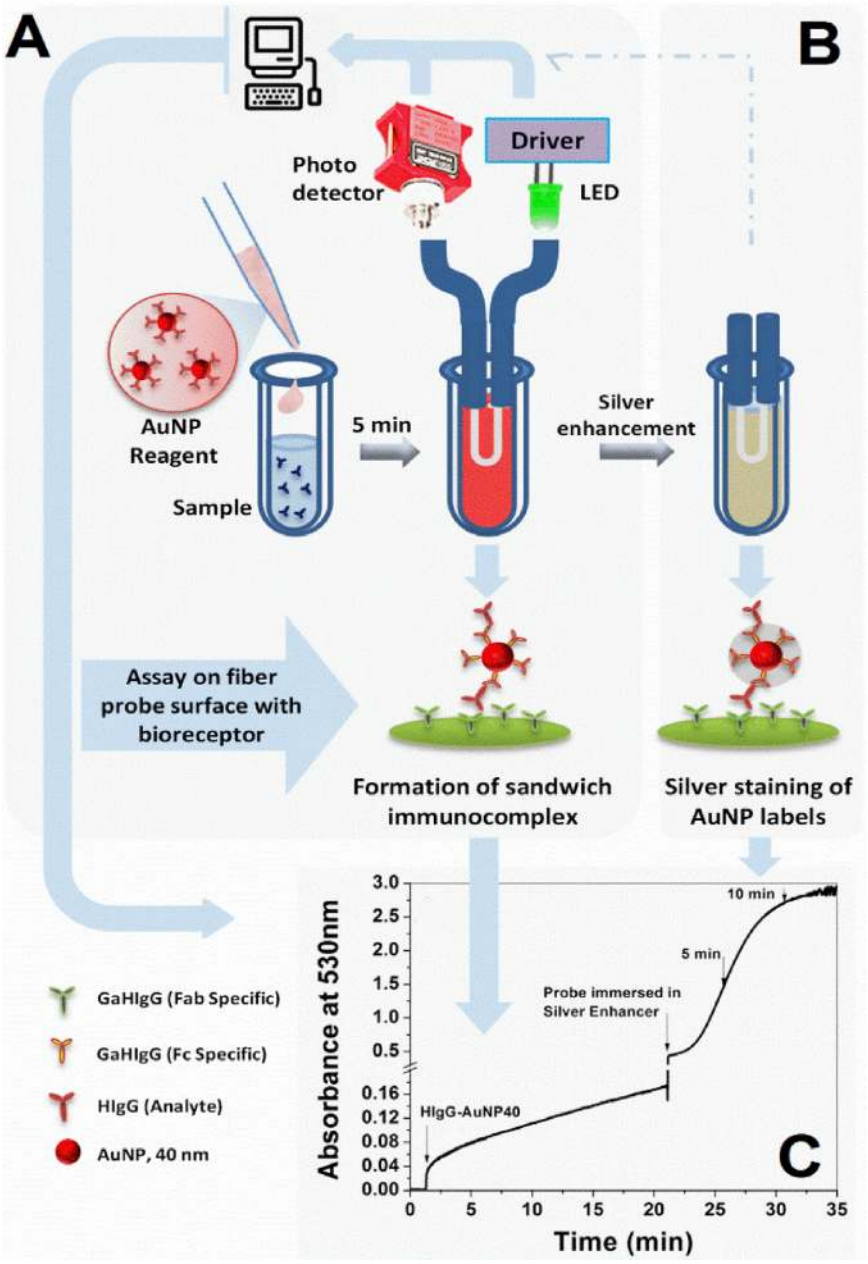

Fig. 2. Schematic showing analyte detection using P-FAB. (A) *Step 1:* A sample solution (25 µL) in a 0.2 mL microcentrifuge tube containing HIgG in phosphate buffer saline (PBS) was mixed with a labelled reagent (25 µL) containing AuNPs conjugated with F_c specific aHIgGs to allow bioaffinity reaction for 5 min. *Step 2:* A U-bent fiberoptic probe coupled between a pair of LED (LED528EHP, 7 mW, Thorlabs Inc. USA) and photodetector (10 pW-50 mW, S150C, Thorlabs Inc., USA) was dipped in the sample-reagent solution. The fiber core was pre-biofunctionalized with aHIgG (F_{ab} specific) antibodies to allow formation of plasmonic sandwich immunocomplex on the probe surface for 20 min. (Note: The distal ends of the fiber probe were connected to LED and PD through bare fiber adaptors and SMA connectors, to avoid bulky optomechanical accessories). (B) The fiber probe was dipped in silver enhancer solution to amplify the plasmonic absorbance signal by catalytic reduction of silver around AuNPs. (C) The sensor response depicted in terms of absorbance by normalizing the optical intensity signal from PD with respect to its initial value at the beginning of the experiment.

obtain dynamic range over the lower analyte concentrations from 1 fg/mL to 100 fg/mL, where the assay with AuNP labels alone lacks enough sensitivity to quantify the analyte.

To benchmark our device, P-FAB results were compared to a standard ELISA and BIAcore 3000 surface plasmon resonance (SPR) system for analyte concentrations between 1 fg/mL and 10 µg/mL. SPR systems are reported to detect such low analyte concentrations by utilizing plasmonic labels [19–21], while analyte concentrations down to 10 ng/mL were detected using ELISA (Fig. S6), BIAcore was more sensitive and able to detect analyte concentration down to 1 fg/mL without any silver enhancement (Figs. 4 and S7). Also, the adaptation of one-step premixed sandwich assay as depicted in Fig. 2A gave rise to a considerably higher absorbance response over a shorter time duration in comparison to the conventional two-step sandwich assay (Fig. S8). Addition of analytical sample to AuNP labelled antibodies prior to exposing them to sensor surface for their detection has two possible advantages including (i) rapid and specific binding of analytes to AuNP labels due to liquid phase reactions [22] and (ii) improvement in diffusion-limited analyte binding kinetics by using AuNP as carriers [23], whose kinetics are known to improve with NP concentrations due to inter-particle repulsive forces at 10× concentration [24]. We anticipate the above two phenomena as responsible for an efficient capture of analyte in the bulk of the liquid phase and transporting them to a sensor surface to potentially aid in significant reduction in LoDs and assay time.

4. Conclusions

The results obtained in this study have multiple important attributes: (i) P-FAB allows rapid dip-type assay for detection of analytes within 25 – 30 min in a small sample volume under static (no-flow) conditions, hence offers compatibility with conventional microcentrifuge tubes and well-plates, (ii) LoDs down to 7 aM can be obtained as shown using low-cost optoelectronic instrumentation, (iii) a wide dynamic range of 7 aM to 7 pM is possible with the help of either bare or silver stained AuNP labels. Further, the versatility of this technique lies in the ability to fine-tune the dynamic range for larger analyte concentrations by tailoring the extinction of plasmonic labels

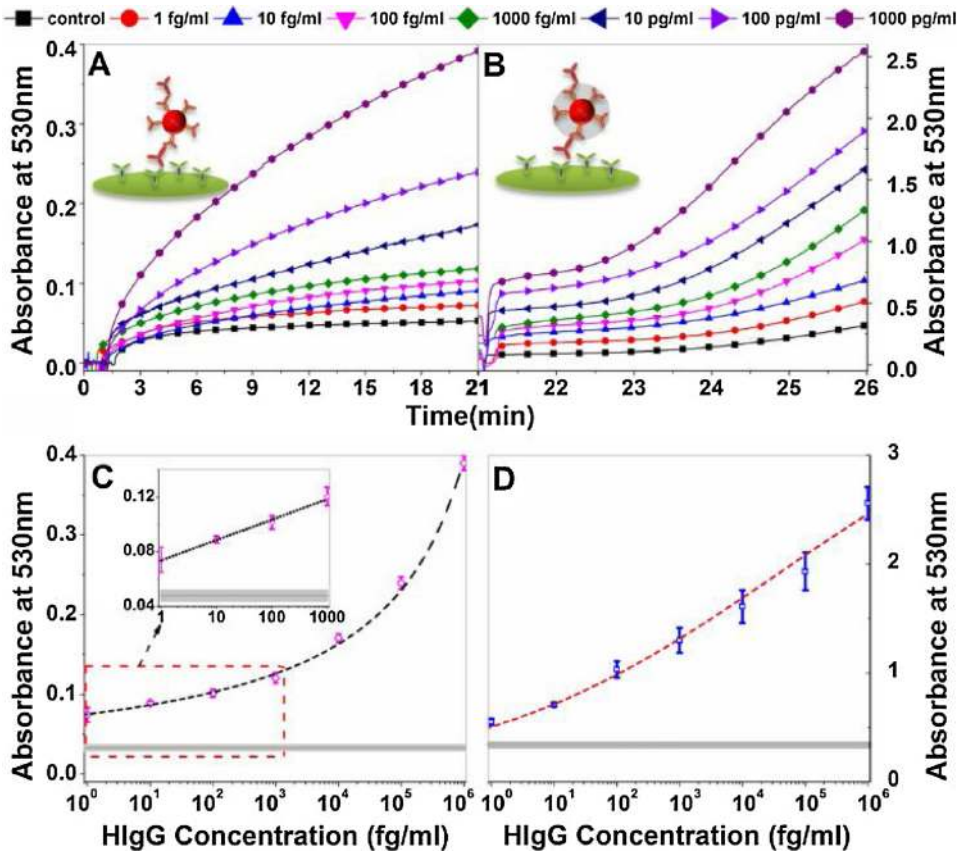

Fig. 3. Detection of ultralow analyte concentrations using P-FAB. (A) Temporal absorbance response curve obtained for U-bent probes due to the formation of plasmonic sandwich immunocomplex (aHIgG-HIgG-aHIgG-AuNP) on the probe fiber surface for HIgG concentrations varying from 1 fg/mL (7 aM) to 1 ng/mL (7 pM). (B) Exponential rise in absorbance response once probes were dipped in silver enhancer solution for 5 min. (C) HIgG dose response curve obtained from a 20 min sandwich assay with 10× NP-aHIgG labels over a dynamic range of 1 fg/mL to 1 ng/mL. Inset: Linear absorbance response (with $R^2 = 0.98$, $n \geq 3$) obtained from log concentrations of 1 fg/mL to 1 pg/mL of HIgG. (D) Dose response curve for the corresponding fiber probes after 5 min of silver enhancement.

(e.g. AuNP < 40 nm) (Fig. S9). A simple cost analysis estimates the fabrication cost of the fiberoptic probes at less than 1 USD each while the optoelectronic instrumentation and optical coupling units used in experiments are portable and cost less than 1000 USD (mainly S150C detector and PM100 console from Thorlabs Inc., which can be replaced with a low-cost PD). The reagents, including antibodies and AuNPs used in the assay cost ~1 USD. Thus, the P-FAB offers ultrahigh sensitivity at a ultralow cost of ~ 2 USD (see SI for detailed calculations). Further optimization of assay protocols and the adoption of an optimally designed microfluidic platform may hopefully lead to detection of ultralow analyte concentrations. It is important to note that the P-FAB relies on accurate measurement of light intensity, which is influenced by the ambient conditions, including temperature and refractive index of the sample-reagent solution. These effects can be compensated by employing a reference probe along with the test probe(s), which may possibly improve the detection limits as well. Owing to the above merits, P-FAB is a highly promising technology for realizing cost-effective, ultrasensitive PoC diagnostics.

CRediT authorship contribution statement

Ramakrishna Bandaru: Conceptualization, Methodology, Investigation, Data curation, Writing - original draft. **Divagar M:** Validation, Writing - original draft. **Shruti Khanna:** Investigation, Data curation, Writing - original draft. **Christina Grace Danny:** Investigation, Data curation, Writing - original draft. **Shalini Gupta:** Supervision, Writing - review & editing. **Vani Janakiraman:** Supervision, Writing - review & editing. **V V R Sai:** Conceptualization, Methodology, Supervision, Writing - review & editing.

Declaration of Competing Interest

The authors declare that they have no known competing financial interests or personal relationships that could have appeared to

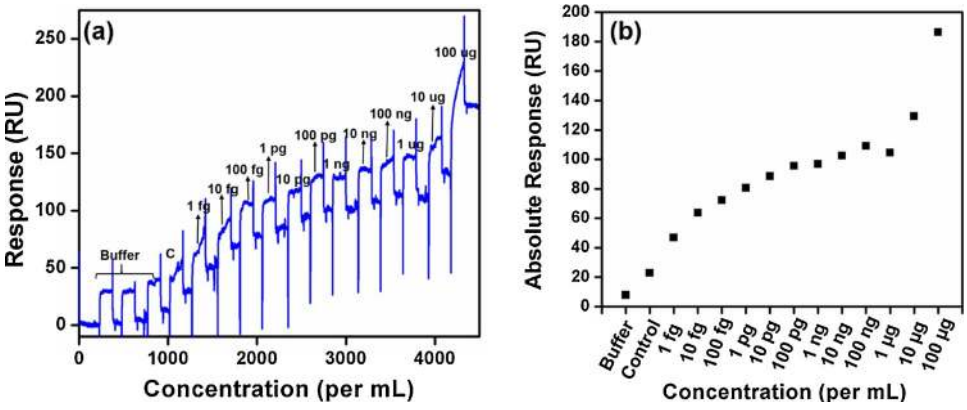

Fig. 4. SPR sensogram showing the (a) association curves of binding affinities for different analyte concentrations with F_{ab} specific aHIgG in a sandwich format (C refers to the control set); (b) absolute binding response obtained by injecting different concentrations of analyte mixed with AuNP reagent showing a concentration-dependent increase in the binding affinity.

influence the work reported in this paper.

Acknowledgments

BR thanks Ministry of Human Resource Development under Government of India, BIRAC-SRISTI, Indo-German Science and Technology (IGSTC) for the partial financial support. VVRS acknowledges the research grant from IIT Madras and IGSTC. DM acknowledges DST INSPIRE PhD Fellowship from the Government of India.

Appendix A. Supplementary data

Supplementary material related to this article can be found, in the online version, at doi:https://doi.org/10.1016/j.snb.2020.128463.

References

[1] S.O. Kelley, C.A. Mirkin, D.R. Walt, R.F. Ismagilov, M. Toner, E.H. Sargent, Advancing the speed, sensitivity and accuracy of biomolecular detection using multi-length-scale engineering, Nat. Nanotechnol. 9 (2014) 969–980, https://doi.org/10.1038/nnano.2014.261.

[2] M. Sajid, A.N. Kawde, M. Daud, Designs, formats and applications of lateral flow assay: a literature review, J. Saudi Chem. Soc. 19 (2015) 689–705, https://doi.org/10.1016/j.jscs.2014.09.001.

[3] G.A. Posthuma-trumpie, J. Korf, Lateral flow (immuno) assay: its strengths, weaknesses, opportunities and threats. A literature survey, Anal. Bioanal. Chem. 393 (2009) 569–582, https://doi.org/10.1007/s00216-008-2287-2.

[4] V.G. Panferov, I.V. Safenkova, N.A. Byzova, Y.A. Varitsev, A.V. Zherdev, B.B. Dzantiev, Silver-enhanced lateral flow immunoassay for highly-sensitive detection of potato leafroll virus, Food Agric. Immunol. 29 (2018) 445–457, https://doi.org/10.1080/09540105.2017.1401044.

[5] H. Ye, X. Xia, Enhancing the sensitivity of colorimetric lateral flow assay (CLFA) through signal amplification techniques, J. Mater. Chem. B. 6 (2018) 7102–7111, https://doi.org/10.1039/C8TB01603H.

[6] J.D. Bishop, H.V. Hsieh, D.J. Gasperino, B.H. Weigl, Sensitivity enhancement in lateral flow assays: a systems perspective, Lab Chip 19 (2019) 2486–2499, https://doi.org/10.1039/c9lc00104b.

[7] L. Anfossi, F. Di Nardo, C. Giovannoli, C. Passini, C. Baggiani, Increased sensitivity of lateral flow immunoassay for ochratoxin A through silver enhancement, Anal. Bioanal. Chem. 405 (2013) 9859–9867, https://doi.org/10.1007/s00216-013-7428-6.

[8] G. Tan, Y. Zhao, M. Wang, X. Chen, B. Wang, Q.X. Li, Ultrasensitive quantitation of imidacloprid in vegetables by colloidal gold and time-resolved fluorescent nanobead traced lateral flow immunoassays, Food Chem. 311 (2020) 126055, https://doi.org/10.1016/j.foodchem.2019.126055.

[9] L. Lu, J. Yu, X. Liu, X. Yang, Z. Zhou, Q. Jin, R. Xiao, C. Wang, Rapid, quantitative and ultra-sensitive detection of cancer biomarker by a SERRS-based lateral flow immunoassay using bovine serum albumin coated Au nanorods, RSC Adv. 10 (2019) 271–281, https://doi.org/10.1039/c9ra09471g.

[10] G. Wu, M.H. Zaman, Low-cost tools for diagnosing and monitoring HIV infection in low-resource settings, Bull. World Health Organ. 90 (2012) 914–920, https://doi.org/10.2471/BLT.12.102780.

[11] B. Ramakrishna, V.V.R. Sai, Evanescent wave absorbance based U-bent fiber probe for immunobiosensor with gold nanoparticle labels, Sens. Actuators B Chem. 226 (2016) 184–190, https://doi.org/10.1016/j.snb.2015.11.107.

[12] M. Divagar, V.V.R. Sai, Fiber optic plasmonic Sandwich immunosensor: influence of AuNP label size and concentration, Proc. IEEE Sensors (2018) 1–4, https://doi.org/10.1109/ICSENS.2018.8589779.

[13] J.W.S. Rayleigh, The problem of the whispering gallery, Philos. Mag. 20 (1910) 1001–1004, https://doi.org/10.1080/14786441008636993.

[14] V.V.R. Sai, T. Kundu, S. Mukherji, Novel U-bent fiber optic probe for localized surface plasmon resonance based biosensor, Biosens. Bioelectron. 24 (2009) 2804–2809, https://doi.org/10.1016/j.bios.2009.02.007.

[15] J. Satija, B. Karunakaran, S. Mukherji, A dendrimer matrix for performance enhancement of evanescent wave absorption-based fiber-optic biosensors, RSC Adv. 4 (2014) 15841–15848, https://doi.org/10.1039/c4ra00198b.

[16] I. Safenkova, A. Zherdev, B. Dzantiev, Factors influencing the detection limit of the lateral-flow sandwich immunoassay: a case study with potato virus X, Anal. Bioanal. Chem. 403 (2012) 1595–1605, https://doi.org/10.1007/s00216-012-5985-8.

[17] S. Amarasiri Fernando, G.S. Wilson, Studies of the “hook” effect in the one-step sandwich immunoassay, J. Immunol. Methods 151 (1992) 47–66, https://doi.org/10.1016/0022-1759(92)90104-2.

[18] S. Gupta, S. Huda, P.K. Kilpatrick, O.D. Velev, Characterization and optimization of gold immunoassays, Anal. Chem. 79 (2007) 3810–3820, https://doi.org/10.1021/ac062341m.

[19] B. Ramakrishna, V. Sai, U-Bent Fiberoptic Evanescent Wave Absorbance Plasmonic Sandwich Biosensor: Silver based Signal Enhancement, 2015 Workshop on Recent Advances in Photonics (WRAP), Bangalore, 2015, pp. 1–4, https://doi.org/10.1109/WRAP.2015.7805978 WRAP2015.

[20] W.C. Law, K.T. Yong, A. Baev, P.N. Prasad, Sensitivity improved surface plasmon resonance biosensor for cancer biomarker detection based on plasmonic enhancement, ACS Nano 5 (2011) 4858–4864, https://doi.org/10.1021/nn2009485.

[21] H.R. Jang, A.W. Wark, S.H. Baek, B.H. Chung, H.J. Lee, Ultrasensitive and ultrawide range detection of a cardiac biomarker on a surface plasmon resonance platform, Anal. Chem. 86 (2014) 814–819, https://doi.org/10.1021/ac4033565.

[22] G.A. Posthuma-Trumpie, J. Korf, A. Van Amerongen, Lateral flow (immuno)assay: its strengths, weaknesses, opportunities and threats. A literature survey, Anal. Bioanal. Chem. 393 (2009) 569–582, https://doi.org/10.1007/s00216-008-2287-2.

[23] T.M. Squires, R.J. Messinger, S.R. Manalis, Making it stick: convection, reaction and diffusion in surface-based biosensors, Nat. Biotechnol. 26 (2008) 417–426, https://doi.org/10.1038/nbt1388.

[24] E. Shahriari, M. Moradi, M. Raeisi, An experimental study of thermal diffusivity of Au nanoparticles: effects of concentration particle size, J. Theor. Appl. Phys. 10 (2016) 259–263, https://doi.org/10.1007/s40094-016-0224-x.